activity of Tat-shepherdin conjugates mediated by co-treatment with Tat-fused endosome-disruptive HA2 peptide. *Biochem Biophys Res Commun* **363**: 1027–1032.

Tyagi M, Rusnati M, Presta M, Giacca M (2001). Internalization of HIV-1 tat requires cell surface heparan sulfate proteoglycans. *J Biol Chem* **276**: 3254–3261.

Wadia JS, Stan RV, Dowdy SF (2004). Transducible TAT-HA fusogenic peptide enhances escape of TAT-fusion proteins after lipid raft macropinocytosis. *Nat Med* **10**: 310–315.

West MA, Bretscher MS, Watts C (1989). Distinct endocytotic pathways in epidermal growth factor-stimulated human carcinoma A431 cells. *J Cell Biol* **109**: 2731–2739.

Yandek LE, Pokorny A, Floren A, Knoelke K, Langel U, Almeida PF (2007). Mechanism of the cell-penetrating peptide transportan 10 permeation of lipid bilayers. *Biophys J* **92**: 2434–2444.

Ziegler A, Seelig J (2004). Interaction of the protein transduction domain of HIV-1 TAT with heparan sulfate: binding mechanism and thermodynamic parameters. *Biophys J* **86**: 254–263.

Journal of Immunological Methods 335 (2008) 71–78

Contents lists available at ScienceDirect

Journal of Immunological Methods

journal homepage: www.elsevier.com/locate/jim

Research paper

Simple and highly sensitive assay system for TNFR2-mediated soluble- and transmembrane-TNF activity

Yasuhiro Abe [a,b], Tomoaki Yoshikawa [a,c], Haruhiko Kamada [a,d], Hiroko Shibata [a,e], Tetsuya Nomura [a,b], Kyoko Minowa [a,f], Hiroyuki Kayamuro [a,b], Kazufumi Katayama [g], Hiroyuki Miyoshi [h], Yohei Mukai [a,b], Yasuo Yoshioka [a,c], Shinsaku Nakagawa [b], Shin-ichi Tsunoda [a,d,*], Yasuo Tsutsumi [a,b,d]

[a] Laboratory of Pharmaceutical Proteomics, National Institute of Biomedical Innovation, 7-6-8 Saito-Asagi, Ibaraki, Osaka 567-0085, Japan
[b] Graduate School of Pharmaceutical Sciences, Osaka University, 1-6 Yamadaoka, Suita, Osaka 565-0871, Japan
[c] The Center for Advanced Research and Education in Drug Discovery and Development, Osaka University, 1-6 Yamadaoka, Suita, Osaka 565-0871, Japan
[d] The Center for Advanced Medical Engineering and Informatics, Osaka University, 1-6 Yamadaoka, Suita, Osaka 565-0871, Japan
[e] Division of Drugs, National Institute of Health Science, 1-18-1 Kamiyoga, Setagaya-ku, Tokyo 158-8501, Japan
[f] Graduate School of Pharmaceutical Sciences, Kyoto Pharmaceutical University, Misasagi-Nakauchicho 5, Yamashina-ku, Kyoto 607-8414, Japan
[g] Allergy & Immunology Project, Tokyo Metropolitan Institute of Medical Science, 3-18-22, Honkomagome, Bunkyo-ku, Tokyo 113-8613, Japan
[h] Subteam for Manipulation of Cell Fate, BioResource Center, RIKEN, 3-1-1 Koyadai, Tsukuba, Ibaraki 305-0074, Japan

ARTICLE INFO

Article history:
Received 25 December 2007
Received in revised form 28 February 2008
Accepted 28 February 2008
Available online 26 March 2008

Keywords:
TNF
TNFR2
Fas
Chimeric receptor
Bioassay

ABSTRACT

Drugs that target tumor necrosis factor-α (TNF) are particularly important in the treatment of severe inflammatory progression in rheumatoid arthritis, Crohn's disease and psoriasis. Despite the central role of the TNF/TNF receptor (TNFR) in various disease states, there is a paucity of information concerning TNFR2 signaling. In this study, we have developed a simple and highly sensitive cell-death based assay system for analyzing TNFR2-mediated bioactivity that can be used to screen for TNFR2-selective drugs. Using a lentiviral vector, a chimeric receptor was engineered from the extracellular and transmembrane domain of human TNFR2 and the intracellular domain of mouse Fas and the recombinant protein was then expressed in TNFR1$^{-/-}$ R2$^{-/-}$ mouse preadipocytes. Our results demonstrate that this chimeric receptor is capable of inducing apoptosis by transmembrane- as well as soluble-TNF stimuli. Moreover, we found that our bioassay based on cell death phenotype had an approximately 80-fold higher sensitivity over existing bioassays. We believe our assay system will be an invaluable research tool for studying TNFR2 and for screening TNFR2-targeted drugs.

1. Introduction

Tumor necrosis factor-α (TNF) is a pleiotropic cytokine that regulates various biological processes such as host defense, inflammation, autoimmunity, apoptosis and tumor cell death through the TNF-receptor 1 (TNFR1) and receptor 2 (TNFR2) (Wajant et al., 2003). TNF/TNFR interaction is considered to be an attractive target for the treatment of refractory diseases, including autoimmune disease and malignant tumors (Aggarwal, 2003; Szlosarek and Balkwill, 2003). In rheumatoid arthritis, for example, biological anti-TNF agents, such as Infliximab and Adalimumab, rapidly reduce signs and symptoms of joint inflammation (Feldmann and Maini, 2003). However, anti-TNF drugs used to treat inflammatory disorders have been reported to increase the risk of infection, in accordance with animal studies (Brown et al., 2002; Nathan et al., 2006).

* Corresponding author. Laboratory of Pharmaceutical Proteomics, National Institute of Biomedical Innovation, 7-6-8 Saito-Asagi, Ibaraki, Osaka 567-0085, Japan. Tel.: +81 72 641 9811x2327; fax: +81 72 641 9817.
E-mail address: tsunoda@nibio.go.jp (S. Tsunoda).

0022-1759/$ – see front matter © 2008 Elsevier B.V. All rights reserved.
doi:10.1016/j.jim.2008.02.019

A thorough understanding of the biology of the TNF/TNFR system is a prerequisite to the safe and effective development of anti-TNF therapeutics. In particular, several factors and mechanisms hypothesized to be involved in the side effects elicited by anti-TNF drugs need to be tested (Curtis et al., 2007; Jacobs et al., 2007; Schneeweiss et al., 2007). These include the differential power of the drugs to neutralize TNF bioavailability and the differential inhibition of TNF signaling events. Despite extensive studies on the molecular biology of TNF/TNFR1 signaling (Micheau and Tschopp, 2003) the functions of TNFR2 are poorly understood. There is an increasing need for a comprehensive understanding of TNF/TNFR2 biology, particularly in terms of the development of TNFR-selective drugs.

In this context, we have used a novel phage-display based screening system (Yamamoto et al., 2003; Shibata et al., 2004, 2008) to develop structural mutants of TNF to help clarify the biology of TNF/TNFR2 interactions. These TNF variants, which exert TNFR2-mediated agonistic or antagonistic activity, might be extremely valuable for elucidating structure-activity relationships between TNF and TNFR2. So far, in order to evaluate the bioactivity of TNF through TNFR2, many researchers have used the TNFR2 over-expressing cell lines (Heller et al., 1992; Weiss et al., 1998), such as rat/mouse T hybridomas transfected with human TNFR2 (PC60-hR2) (Vandenabeele et al., 1992). The PC60-hR2 assay is based on granulocyte macrophage colony-stimulating factor (GM-CSF) secretion mediated by TNF/TNFR2 stimuli. The GM-CSF secretion level is quantified by proliferation of GM-CSF-dependent cell lines or by ELISA. However, this two-step assay system is complicated and the screening process is highly laborious. Thus, there are increasing demands for the development of a simple, highly sensitive screening system that is TNFR2-selective.

In the present study, we developed a simple but highly sensitive cell death-based assay system for evaluating TNFR2-mediated activity. We constructed a lentiviral vector expressing a chimeric receptor derived from the extracellular (EC) and transmembrane (TM) domain of human TNFR2 (hTNFR2) and the intracellular (IC) domain of mouse Fas (mFas). Additionally, to eliminate the influence of the endogenous TNFR1, the chimeric receptor was expressed on TNFR1$^{-/-}$R2$^{-/-}$ preadipocytes (Xu et al., 1999). We found that hTNFR2/mFas-expressing preadipocyte (hTNFR2/mFas-PA) showed about 80-times higher sensitivity after treatment with soluble-TNF and over the conventional method. Furthermore, hTNFR2/mFas-PA could detect not only transmembrane TNF- (tmTNF) but also soluble TNF-activity. The technology described herein will be highly useful both as an assay system for various TNF variants *via* TNFR2 and also as a cell-based drug discovery system for TNFR2 agonists/antagonists.

2. Materials and methods

2.1. Cell culture

TNFR1$^{-/-}$R2$^{-/-}$, TNFR1$^{-/-}$, and wild-type (wt) preadipocytes established from day 16–17 mouse embryos were generously provided by Dr. Hotamisligil (Harvard School of Public Health, Boston MA). Preadipocytes, 293T cells and HeLaP4 cells were cultured in Dulbecco's modified Eagle's medium (DMEM; Sigma-Aldrich, Inc., Tokyo, Japan) with 10% bovine fetal serum (FBS) and 1% antibiotic cocktail (penicillin 10,000 u/ml, streptomycin 10 mg/ml, and amphotericin B 25 μg/ml; Nacalai Tesque, Kyoto, Japan). The rat/mouse T hybridomas PC60-hR2 cells (hTNFR2 transfected PC60 cells) were generously provided by Dr. Vandenabeele (University of Gent, Belgium) and cultured in RPMI 1640 (Sigma-Aldrich, Inc.) with 10% FBS, 1 mM sodium pyrubate, 5×10^{-5} M 2-ME, 3 μg/ml puromycin (Wako Pure Chemical Industries, Osaka, Japan), and 1% antibiotic cocktail. TNFR1$^{-/-}$R2$^{-/-}$ mouse macrophages were generously provided by Dr. Aggarwal (University of Texas MD Anderson Cancer Center, Houston, TX), and cultured in RPMI 1640 with 10% FBS and 1% antibiotic cocktail.

2.2. Construction of self-inactivating (SIN) lentiviral vector

Vectors were constructed using standard cloning procedures. A DNA fragment encoding the EC and TM parts of hTNFR2 was amplified by polymerase chain reaction (PCR) from human peripheral blood lymphocyte cDNA with the following primer pairs: forward primer (5′-GAT TAC GCC AAG CTT GTC GAC CAC CAT GGC GCC CGT CGC CGT CTG GGC CGC GCT GGC CGT CGG ACT GGA G-3′) containing a SalI site at the 5′-end and a reverse primer (5′-CAC CTT GGC TTC TCT CTG CTT TCG AAG GGG CTT CTT TTT CAC CTG GGT CA-3′) containing a Csp45I site. The resulting amplified fragment was subcloned into pCR-Blunt II-TOPO (Invitrogen Corp., Carlsbad, CA) to generate pCR-Blunt-hTNFR2. A fragment encoding the IC domain of mFas was amplified by PCR from mouse spleen cDNA with the following primer pair: forward primer (5′-AAT TCC ACT TGT ATT TAT ACT TCG AAA GTA CCG GAA AAG A-3′) containing a Csp45I site and a reverse primer (5′-GTC ATC CTT GTA GTC TGC GGC CGC TCA CTC CAG ACA TTG TCC TTC ATT TTC ATT TCC A-3′) containing a NotI site at the 5′-end. The mFas DNA fragment was subcloned into pCR-Blunt-hTNFR2 between the Csp45I and NotI sites to combine the EC and TM domains of hTNFR2 to the IC domains of mFas, generating pCR-Blunt-hTNFR2/mFas (Fig. 1A). Then the hTNFR2/mFas DNA fragment was cloned between the XhoI and NotI sites of SIN lentiviral vector construct, which contains the blasticidin (Bsd) resistance gene, generating CSII-CMV-hTNFR2/mFas-IRES2-Bsd (Fig. 1B). For construct tmTNF, a DNA fragment encoding non-cleavable human tmTNF h(tmTNFΔ1-12), generated by deleting amino acids 1–12 in the N-terminal part of hTNF, was amplified by PCR from hTNF cDNA with following primer pair: forward primer (5′-AGT GAT CGG CCC CCA GAG GGA AGC TTA GAT CTC TCT CTA ATC AGC CCT CTG GCC CAG GCA GTA GCC CAT GTT GTA GCA AAC CCT CAA G-3′) and reverse primer (5′-GGT TGG ATG TTC GTC CTC CGC GGC CGC CTA ACT AGT TCA CAG GGC AAT GAT CCC AAA GTA GAC CTG-3′) and cloned into the pY03′ vector. Then tmTNFΔ1–12 DNA fragment was cloned between the SalI and XhoI sites of the SIN vector construct, generating CSII-EF-tmTNF-IRES-GFP.

2.3. Preparation of lentiviral vectors

The method used to prepare the lentiviral vector has been described previously (Miyoshi et al., 1999; Katayama et al.,

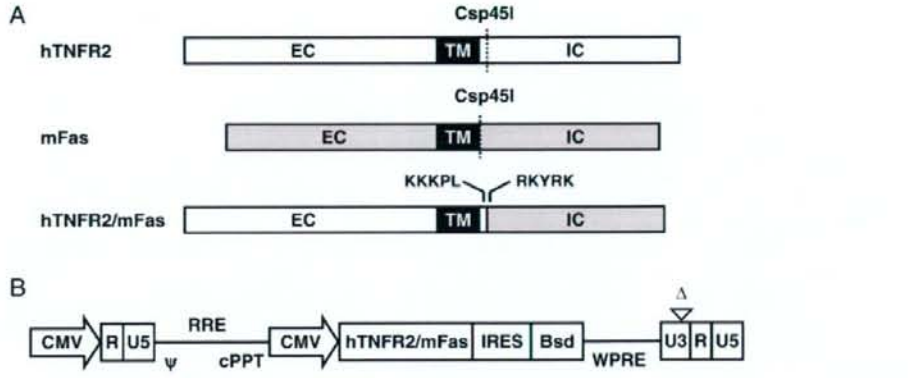

Fig. 1. Construction of hTNFR2/mFas chimeric receptor gene and vector. (A) The cDNA structures of hTNFR2, mFas and fusion genes (hTNFR2/mFas) are shown. EC: extracellular domain, TM: transmembrane domain, IC: Intracellular domain. (B) Schematic representation of self-inactivating (SIN) LV plasmid (CSII-CMV-hTNFR2/mFas-IRES-Bsd). CMV, cytomegalovirus promoter; ψ: packaging signal; RRE, rev responsive element; cPPT, central polypurine tract; IRES, Encephalomyocarditis virus internal ribosomal entry site; Bsd, Blasticidin; WPRE, woodchuck hepatitis virus posttranscriptional regulatory element. Δ: deleting 133 bp in the U3 region of the 3′ long terminal repeat.

2004). In brief, 293T cells were transfected by the calcium phosphate method with three plasmids: packaging construct (pCAG-HIVgp), VSV-G and Rev expressing construct (pCMV-VSV-G-RSV-Rev) and SIN vector construct (CSII-CMV-TNFR2/Fas-IRES2-Bsd or CSII-EF-tmTNF-IRES-GFP). Two days after transfection, the conditioned medium was collected and the virus was concentrated by ultracentrifugation at 50,000 × g for 2 h at 20 °C. The pelleted virus was resuspended in Hanks' balanced salt solution (GIBCO BRL, Paisley, UK). Vector titers were determined by measuring the infectivity of HeLaP4 cells with serial dilutions of vector stocks using flow cytometric analysis (FCM) for hTNFR2/mFas- or GFP-positive cells.

2.4. Preparation of hTNFR2/mFas- or tmTNF-expressing cell culture

To prepare the hTNFR2/mFas- or tmTNF-expressing cell culture, $TNFR1^{-/-}R2^{-/-}$ preadipocytes or $TNFR1^{-/-}R2^{-/-}$ macrophages were infected with each lentiviral vector at a multiplicity of infection (MOI) of 100. Stable hTNFR2/mFas-transfectants were selected for growth in culture medium containing 8 μg/ml Bsd (Invitrogen Corp.) for 1 week. Expression of hTNFR2/mFas chimeric receptor on Bsd-resistant cells was detected by staining with biotinylated anti-hTNFR2 antibody (BD Biosciences, Franklin Lakes, NJ) at 0.5 μg/5×10^5 cells for 30 min at 4 °C. Subsequently, the cells were washed and stained with streptavidin-PE conjugate (BD Biosciences). The cell suspension was centrifuged at 800 × g, washed with PBS, centrifuged again, and then re-suspended in 500 μl of 0.4% paraformaldehyde. Fluorescence was analyzed on a FACS Vantage flow cytometer, and data were analyzed using CellQuest software (both BD Biosciences). The hTNFR2/mFas-positive cell cultures were used in subsequent experiments as hTNFR2/mFas-PA cells. For preparation of tmTNF-expressing $TNFR1^{-/-}R2^{-/-}$ macrophages (tmTNF-Mφ), IRES-driven GFP positive cells were sorted by FACSAria (BD Biosciences).

2.5. Cytotoxicity assays

Cells were seeded on 96-well micro titer plates at a density of 1.5×10^4 cells/well in culture medium. Serial dilutions of mouse or human TNF (mTNF or hTNF; Peprotech, Rocky Hill, NJ), anti-mFas antibody (clone Jo2; BD Biosciences), or paraformaldehyde-fixed tmTNF-Mφ were prepared with DMEM containing 1 μg/ml cycloheximide, and added to each well. After 48 h incubation, the cell viability was measured by WST-8 assay kit (Nacalai Tesque) according to the manufacturer's instructions. The assay is based on cleavage of the tetrazolium salt WST-8 to formazan by cellular mitochondrial dehydrogenase.

2.6. Induction of GM-CSF secretion on PC60-hR2

5×10^4 of PC60-hR2 cells were seeded on a 96 well plate and then exposed to a serial dilution of hTNF in the presence of IL-1β (2 ng/ml). After 24 h incubation, hTNFR2-mediated GM-CSF secretion on PC60-hR2 cells was quantified by ELISA kit according to the manufacturer's protocol (R&D Systems, Minneapolis, MN).

2.7. Immunoprecipitation and western blotting

For immunoprecipitation we used FLAG-TNF (a FLAG-tag fusion protein of hTNF), which was generated in *E. coli* and purified in our laboratory. The protocol for the expression and purification of recombinant proteins has been described previously (Yamamoto et al., 2003). 1×10^7 hTNFR2/mFas-PA cells were treated with or without 100 ng/ml of FLAG-TNF for 30 min at 37 °C. Cells were then harvested and lysed in 1 ml of lysis buffer (50 mM Tris HCl, pH 7.4, 150 mM NaCl, 1% Triton X-100, 1 mM EDTA and protease inhibitor cocktail; Sigma-Aldrich Inc.) and gently rocked at 4 °C for 30 min. Cell debris was removed by centrifugation at 10,000 ×g for 30 min. The resulting supernatant was immunoprecipitated with anti-FLAG-M2 affinity beads (Sigma, St.Louis, MO) for 4 h at 4 °C. Immune complexes bound to the beads were washed three

times with 500 μl of lysis buffer and eluted with 3×FLAG peptide at a concentration of 150 ng/ml. Collected proteins were resolved on 10–20% SDS-PAGE gels and transferred to polyvinylidene fluoride membranes (Millipore Corp., Billerica, MA) by electroblotting. Western blot analyses were performed with biotinylated anti-hTNFR2 antibody (R&D systems) or anti-FADD (Fas-associated death domain protein) antibody (H-181; Santa Cruz Biotechnology Inc., Santa Cruz, CA). Bound primary antibodies were visualized with horseradish peroxidase-conjugated streptavidin or goat-anti-rabbit-IgG (Jackson Immunoresearch Lab., West Grove, PA) respectively, and ECL plus western blotting detection reagents (GE Healthcare, Buckinghamshire, UK). A LAS 3000 image analyzer (Fujifilm, Tokyo, Japan) was used for the observation of chemiluminescence.

3. Results

3.1. Fas- but not TNFR-mediates induction of cell-death in $TNFR1^{-/-}R2^{-/-}$ preadipocytes

Initially, we established a cell line that could be used to evaluate TNFR2-specific bioactivity by means of the chimeric receptor (hTNFR2/mFas) strategy. The parental cell line must

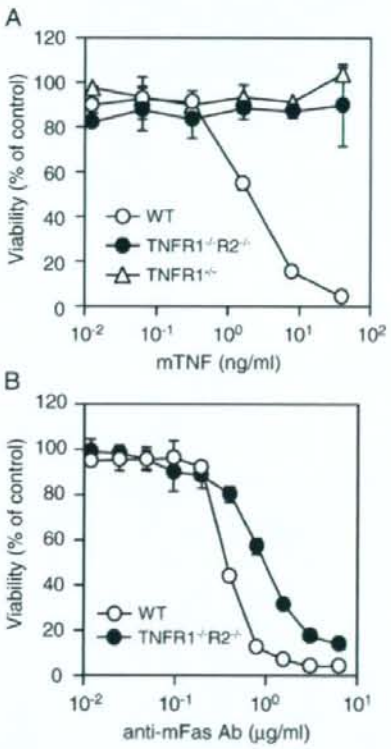

Fig. 2. Fas, but not TNFR2, induced cell death in preadipocytes. WT, $TNFR1^{-/-}R2^{-/-}$ and $TNFR1^{-/-}$ cells were treated with serial dilutions of (A) mTNF or (B) anti-mFas Ab. Cell viability was determined using the WST-8 Assay. Each data point represents the mean ± SD of triplicate wells.

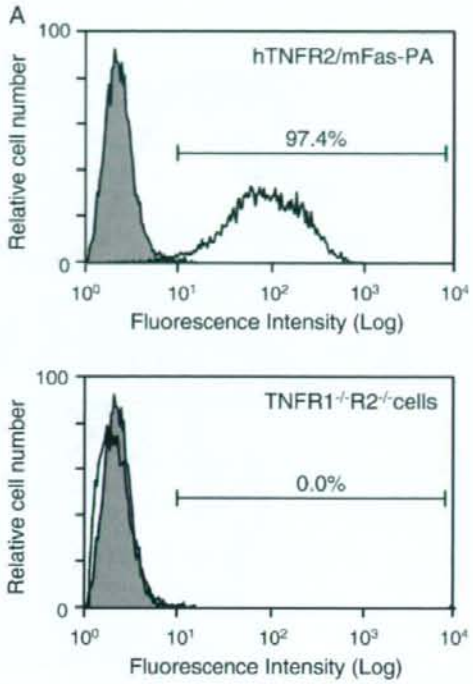

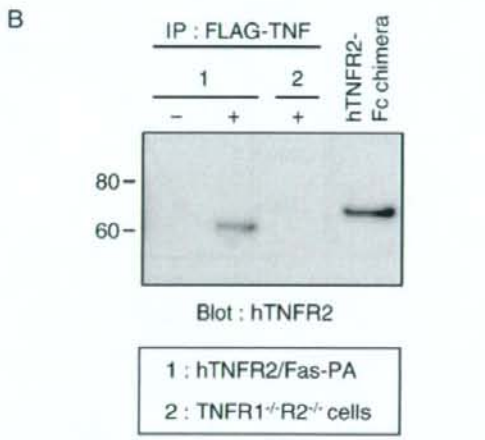

Fig. 3. Expression of hTNF2/mFas chimeric receptor on transfectants. (A) Expression of the chimeric receptor on hTNFR2/mFas-PA (upper panel) or parental $TNFR1^{-/-}R2^{-/-}$ cells (lower panel) was analyzed by flow cytometry using hTNFR2-specific antibody (open histograms) or isotype control antibody (shaded histograms). (B) hTNFR2/mFas-PA or $TNFR1^{-/-}R2^{-/-}$ cells were treated (+) with FLAG-TNF; (−) denotes untreated control cells. Immunoprecipitation was performed with anti-FLAG antibody M2-conjugated beads. After extensive washing, the immunocomplexes were eluted with 3×FLAG peptide. Eluted proteins were resolved on 10–20% SDS-PAGE gels and the presence of hTNFR2/mFas in the complex was detected by western blot using anti-hTNFR2 antibody.

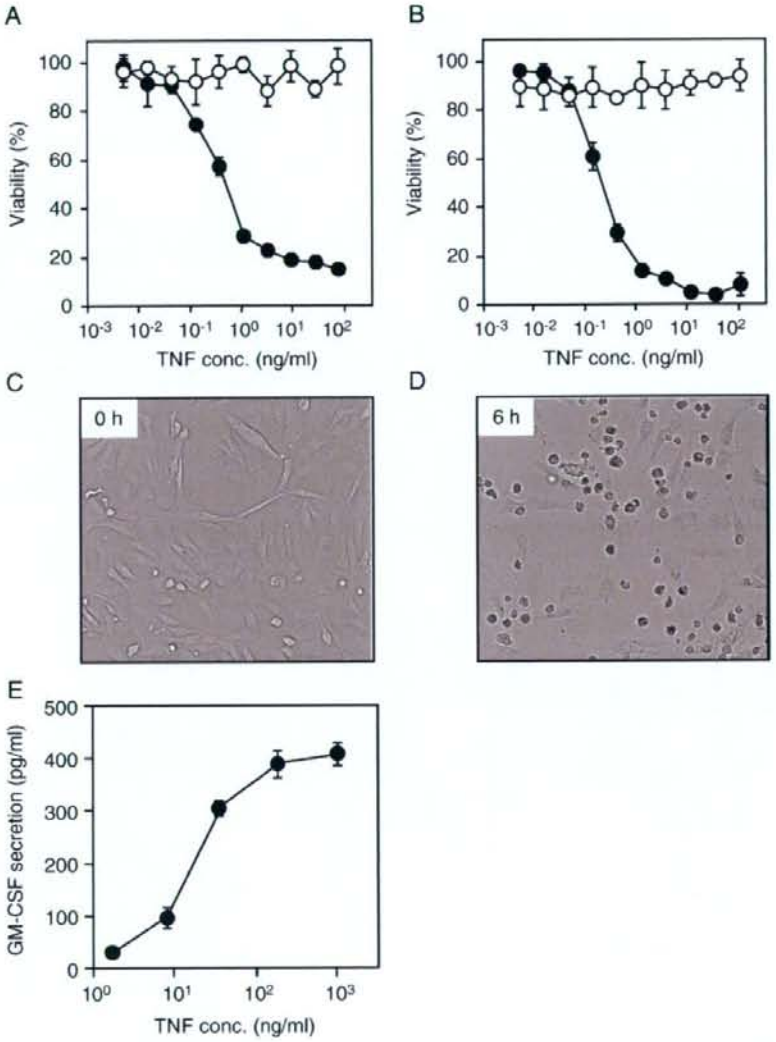

Fig. 4. Induction of strong cell death on hTNFR2/mFas-PA by soluble hTNF. hTNFR2/mFas-PA (●) and parental TNFR1$^{-/-}$R2$^{-/-}$ (○) cells were treated with serial dilutions of hTNF in the presence of cycloheximide (1 μg/ml). After (A) 24 h and (B) 48 h, the cell viability was measured using the WST-8 Assay. Data from the WST-8 assay represents the mean and SDs of triplicate assays. Similar results were obtained in three independent experiments. (C) Untreated or (D) hTNF-treated (10 ng/ml) hTNFR2/mFas-PA cells were incubated for 6 h, and were assessed by light microscopy. (E) PC60-hR2 cells were incubated in the presence of a serial dilution of hTNF and IL-1β (2 ng/ml). After 24 h, induction of GM-CSF was determined by ELISA. Each data point represents the mean±SD of triplicate measurements.

possess both Fas-sensitivity and TNF-resistance. Thus, we selected TNFR1$^{-/-}$R2$^{-/-}$ preadipocytes as the parental cell line and then examined the susceptibility of this cell line against TNFR1- and Fas-induced cell death. TNFR1$^{-/-}$R2$^{-/-}$ preadipocytes were resistant to TNF-induced cell death, while WT preadipocytes, which co-express both TNFR1 and TNFR2, were killed by mTNF-treatment in a dose-dependent manner (Fig. 2A). TNFR1$^{-/-}$ preadipocytes were also resistant to TNF-induced cell death. Thus, TNF-mediated cell death is presumably due to TNFR1-stimuli in accordance with previous reports (Vandenabeele et al., 1995; Ashkenazi and Dixit, 1998; Devin et al., 2000). Anti-Fas antibody treatment induced cell death for both WT, R1$^{-/-}$ and TNFR1$^{-/-}$R2$^{-/-}$ preadipocytes (Fig. 2B). Based on these results, we therefore selected TNFR1$^{-/-}$R2$^{-/-}$ preadipocytes for constructing an hTNFR2/mFas-expressing cell line.

3.2. hTNFR2-expression analysis of LV-hTNFR2/mFas-Bsd infected Bsd-resistant cells

Using the LV technique followed by Bsd selection, we established transfectants that stably expressed hTNFR2/mFas chimeric receptor in which the EC and TM portion of hTNFR2 (amino acids 1–292) was fused to the IC region of mFas (amino acids 187–328) (Figs. 1A and B). FCM analysis revealed that almost 95% of Bsd-resistant cells expressed the EC domain of hTNFR2 (Fig. 3A). To determine whether hTNFR2/mFas retained binding activity against hTNF, we next performed immunoprecipitation and western blot analysis (Fig. 3B). These analyses showed that FLAG-TNFs were immunoprecipitated and eluted with hTNFR2/mFas from LV-transfected and Bsd-resistant cells, but not from parental TNFR1$^{-/-}$R2$^{-/-}$ preadipocytes and untreated cells. Thus, we succeeded in constructing hTNFR2/mFas expressing TNFR1$^{-/-}$ R2$^{-/-}$ preadipocytes that retained the ability to bind hTNF.

3.3. Induction of apoptosis on hTNFR2/mFas-PA

To examine whether the death signal could be transduced by stimulating the chimeric receptors, we evaluated the cell viability of soluble hTNF-treated hTNFR2/mFas-PA. As anticipated, addition of hTNF to hTNFR2/mFas-PA induced a strong cytotoxic effect 24 and 48 h later, whereas no cell death was detected using parental TNFR1$^{-/-}$R2$^{-/-}$ preadipocytes (Figs. 4A and B). After 48 h, more than 90% of hTNFR2/mFas-PA cells were killed by hTNF at a concentration of 4 ng/ml, resulting in a median effective concentration (EC50) of 250 pg/ml. The images in Figs. 4C and D show that hTNFR2/mFas-PA cells underwent clear morphological changes, indicating apoptosis by hTNF stimuli. Additionally, PC60-hR2 cells were tested for hTNFR2-mediated GM-CSF secretion (Fig. 4E). The concentration required to induce 50% of maximal secretion of GM-CSF obtained with hTNF (EC50) was approximately 20 ng/ml. Importantly, our bioassay based on cell death phenotype displayed a ~80-fold higher level of sensitivity over conventional methodologies. Moreover, tmTNF (Fig. 5) and anti-TNFR2 agonistic antibody (data not shown) induced hTNFR2/mFas-PA cell death.

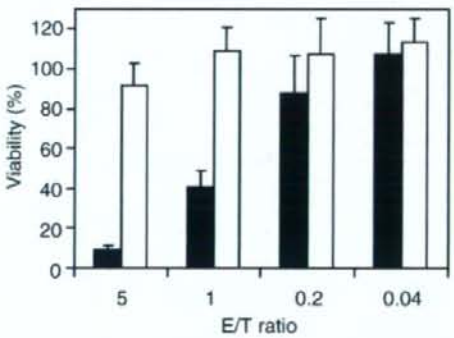

Fig. 5. hTNFR2/mFas-PA cells could be induced cell death by tmTNF. hTNFR2/mFas-PA cells were co-incubated with paraformaldehyde-fixed tmTNF-Mϕ (filled bars) or TNFR1$^{-/-}$ R2$^{-/-}$ Mϕ (open bars) at an effector/target (E/T) ratio of 5:1, 1:1, 0.2:1 and 0.4:1 in the presence of cycloheximide (1 μg/ml). After 48 h, cell viability was measured by WST-8 Assay. Each data point represents the mean ± SD of triplicate measurements.

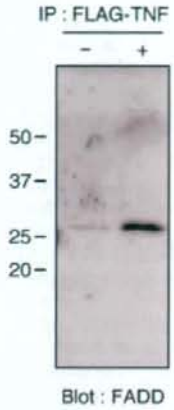

Fig. 6. Recruitment of FADD to the hTNFR2/mFas chimeric receptor in response to hTNF. hTNFR2/mFas-PA or TNFR1$^{-/-}$ R2$^{-/-}$ cells were treated (+) with FLAG-TNF; (–) denotes untreated cells. Immunoprecipitation was performed with anti-FLAG antibody M2-conjugated beads. After extensive washing, immunocomplexes were eluted with 3×FLAG peptide. The eluted proteins were resolved on 10–20% SDS-PAGE gels and the presence of hTNFR2/mFas in the complex was detected by western blot using anti-FADD Antibody.

3.4. Recruitment of FADD to the hTNFR2/mFas chimeric receptor

Recent studies indicate that some TNFR family members, including Fas, self-associate as trimers prior to ligand binding. Activation of the pre-associated receptors is triggered by ligand-induced rearrangement of the assembled trimers (Algeciras-Schimnich et al., 2002). We speculated that the first reaction after ligand-induced oligomerization of hTNFR2/mFas might be the recruitment of FADD, leading to caspase-8 activation. To investigate the composition of the ligand-hTNFR2/mFas signaling complex, we treated hTNFR2/mFas-PA cells with FLAG-tagged hTNF and affinity purified the receptor complex using anti-FLAG antibody-conjugated beads, followed by western blot analysis with antibody against FADD. As expected, FADD was immunoprecipitated with hTNFR2/mFas on hTNF-treated hTNFR2/mFas-PA (Fig. 6). In similar experiments, we could not detect TRADD, which is recruited to TNFR1 in a ligand-dependent process (data not shown). It has been reported that, in contrast to TNFR1, Fas does not interact with TRADD but directly recruits FADD, leading to efficient cell death (Stanger et al., 1995; Dempsey et al., 2003). Because hTNFR2/mFas interacts with FADD, our hTNFR2/mFas-PA cell-based assay system will be useful for evaluating hTNF activity specifically *via* hTNFR2.

4. Discussion

Here, we developed a hTNFR2/mFas-PA cell-based assay system in order to investigate hTNF activity through hTNFR2. The assay is simple to perform and can detect hTNF-mediated hTNFR2 activity with high sensitivity. Because the hTNFR2/

mFas-PA system was engineered in TNFR1$^{-/-}$R2$^{-/-}$ preadipocytes, we were able to analyze hTNF-mediated hTNFR2 activity without affecting TNFR1-related apoptosis. Moreover, not only tmTNF- but also soluble TNF-mediated hTNFR2 activity was detectable using the hTNFR2/mFas-PA cell system.

In our system, hTNFR2-mediated cytotoxic activity on hTNFR2/mFas-PA cells was quantitatively determined using the WST-8 assay. Alternative methods, such as the MTT assay or Methylene Blue assay, are also capable of detecting cytotoxicity. Using the WST-8 assay, hTNFR2-mediated cytotoxic activity was readily detected 24 h after hTNF treatment (Fig. 4A), although a stronger signal was generated with a longer incubation time (48 h; Fig. 4B). Therefore, 48 h-treatment might be more appropriate for evaluating the activity of a low dose of hTNF or when analyzing an activity-weakened mutant TNF. Furthermore, if you evaluate in the absence of CHX, it may be desirable to alter the cell numbers from 1.5 to 1.0×10^4 cells/well. Previously, a similar assay system to the one described in this report was developed by Heidenreich et al. based on murine TNFR1$^{-/-}$R2$^{-/-}$ cells, which heterogenetically expressed human Fas conjugated with hTNFR2 (termed MF-R2-Fas cells) (Krippner-Heidenreich et al., 2002). However, there are some important differences between the MF-R2-Fas cells and the cell line used in our assay system (hTNFR2/mFas-PA), such as detachability. Surprisingly, unlike MF-R2-Fas cells, hTNFR2/mFas-PA cells can detect tmTNF-mediated activity as well as soluble TNF activity. Currently, the reason for this difference is unclear, although it may be caused by heterogeneity of the Fas domain. Indeed, the genetic homology between murine Fas and human Fas in IC domain is approximately 50%. Additionally, other factors may account for the observed differences between the two assay systems, such as expression level of the chimeric receptor. At any event, our results suggest that hTNFR2/mFas-PA cells will be useful in providing the basis for a highly sensitive assay system for analyzing hTNFR2 activity mediated by both soluble TNF and tmTNF. We are currently attempting to generate a TNFR2-selective mutant TNF using this assay system and a phage display system for TNF-therapy or anti-TNF therapy (unpublished data). We chose to use hTNFR2/mFas-PA cells in the screening process for a TNFR2-selective mutant TNF because this cell line is sensitive against not only purified TNF but also culture supernatants of TNF-transfected *E. coli* (crude samples). Therefore, our simple and sensitive bioassay enables high-throughput screening for TNFR2-selective mutant TNFs. The TNFR2-selective mutant will make it possible to perform a structure-function study of TNF/TNFR at any stage of function.

With the success of the human genome project, the focus of life science research has shifted to functional and structural analyses of proteins, such as disease proteomics (Oh et al., 2004; Gilchrist et al., 2006). Thus, there is increasing expectation on drug discovery/development based on the information from genomics or proteomics research, structural biology studies, or receptor-ligand interaction analyses. In particular, the therapeutic application of bioactive proteins, such as cytokines and the newly identified ligand proteins, is eagerly awaited (Gollob et al., 2003; Ansell et al., 2006). Surprisingly, however, these ligand proteins display multiple functions, which has severely limited their clinical application (Margolin et al., 1994; Eskander et al., 1997). Because the reason behind this limitation is that these ligand proteins stimulate different signal transduction pathways via multiple (two or more) receptors, the discovery of receptor-specific agonistic or antagonistic drugs is keenly awaited. Our assay system using a chimeric receptor strategy is applicable to other cytokines and thereby provides a new avenue for identifying receptor-specific agonists or antagonists. We fully anticipate that our novel technology will accelerate the development of TNFR2-related therapeutic molecules as well as acting as a research tool for studying the biology of TNFR2.

Acknowledgements

This study was supported in part by Grants-in-Aid for Scientific Research (No. 18015055, 17689008) from the Ministry of Education, Culture, Sports, Science and Technology of Japan, in part by Health Labor Sciences Research Grant from the Ministry of Health, Labor and Welfare of Japan, in part by Health Sciences Research Grants for Research on Health Sciences focusing on Drug Innovation from the Japan Health Sciences Foundation, and in part by JSPS Research Fellowships for Young Scientists from the Japan Society for the Promotion of Science.

References

Aggarwal, B.B., 2003. Signalling pathways of the TNF superfamily: a double-edged sword. Nat. Rev. Immunol. 3, 745.

Algeciras-Schimnich, A., Shen, L., Barnhart, B.C., Murmann, A.E., Burkhardt, J.K., Peter, M.E., 2002. Molecular ordering of the initial signaling events of CD95. Mol. Cell Biol. 22, 207.

Ansell, S.M., Geyer, S.M., Maurer, M.J., Kurtin, P.J., Micallef, I.N., Stella, P., Etzell, P., Novak, A.J., Erlichman, C., Witzig, T.E., 2006. Randomized phase II study of interleukin-12 in combination with rituximab in previously treated non-Hodgkin's lymphoma patients. Clin. Cancer Res. 12, 6056.

Ashkenazi, A., Dixit, V.M., 1998. Death receptors: signaling and modulation. Science 281, 1305.

Brown, S.L., Greene, M.H., Gershon, S.K., Edwards, E.T., Braun, M.M., 2002. Tumor necrosis factor antagonist therapy and lymphoma development: twenty-six cases reported to the Food and Drug Administration. Arthritis Rheum. 46, 3151.

Curtis, J.R., Patkar, N., Xie, A., Martin, C., Allison, J.J., Saag, M., Shatin, D., Saag, K.G., 2007. Risk of serious bacterial infections among rheumatoid arthritis patients exposed to tumor necrosis factor alpha antagonists. Arthritis Rheum. 56, 1125.

Dempsey, P.W., Doyle, S.E., He, J.Q., Cheng, G., 2003. The signaling adaptors and pathways activated by TNF superfamily. Cytokine Growth Factor Rev. 14, 193.

Devin, A., Cook, A., Lin, Y., Rodriguez, Y., Kelliher, M., Liu, Z., 2000. The distinct roles of TRAF2 and RIP in IKK activation by TNF-R1: TRAF2 recruits IKK to TNF-R1 while RIP mediates IKK activation. Immunity 12, 419.

Eskander, E.D., Harvey, H.A., Givant, E., Lipton, A., 1997. Phase I study combining tumor necrosis factor with interferon-alpha and interleukin-2. Am. J. Clin. Oncol. 20, 511.

Feldmann, M., Maini, R.N., 2003. Lasker Clinical Medical Research Award. TNF defined as a therapeutic target for rheumatoid arthritis and other autoimmune diseases. Nat. Med. 9, 1245.

Gilchrist, A., Au, C.E., Hiding, J., Bell, A.W., Fernandez-Rodriguez, J., Lesimple, S., Nagaya, H., Roy, L., Gosline, S.J., Hallett, M., Paiement, J., Kearney, R.E., Nilsson, T., Bergeron, J.J., 2006. Quantitative proteomics analysis of the secretory pathway. Cell 127, 1265.

Gollob, J.A., Veenstra, K.G., Parker, R.A., Mier, J.W., McDermott, D.F., Clancy, D., Tutin, L., Koon, H., Atkins, M.B., 2003. Phase I trial of concurrent twice-weekly recombinant human interleukin-12 plus low-dose IL-2 in patients with melanoma or renal cell carcinoma. J. Clin. Oncol. 21, 2564.

Heller, R.A., Song, K., Fan, N., Chang, D.J., 1992. The p70 tumor necrosis factor receptor mediates cytotoxicity. Cell 70, 47.

Jacobs, M., Togbe, D., Fremond, C., Samarina, A., Allie, N., Botha, T., Carlos, D., Parida, S.K., Grivennikov, S., Nedospasov, S., Monteiro, A., Le Bert, M.,

Quesniaux, V., Ryffel, B., 2007. Tumor necrosis factor is critical to control tuberculosis infection. Microbes Infect. 9, 623.
Katayama, K., Wada, K., Miyoshi, H., Ohashi, K., Tachibana, M., Furuki, R., Mizuguchi, H., Hayakawa, T., Nakajima, A., Kadowaki, T., Tsutsumi, Y., Nakagawa, S., Kamisaki, Y., Mayumi, T., 2004. RNA interfering approach for clarifying the PPARgamma pathway using lentiviral vector expressing short hairpin RNA. FEBS Lett. 560, 178.
Krippner-Heidenreich, A., Tubing, F., Bryde, S., Willi, S., Zimmermann, G., Scheurich, P., 2002. Control of receptor-induced signaling complex formation by the kinetics of ligand/receptor interaction. J. Biol. Chem. 277, 44155.
Margolin, K., Aronson, F.R., Sznol, M., Atkins, M.B., Gucalp, R., Fisher, R.I., Sunderland, M., Doroshow, J.H., Ernest, M.L., Mier, J.W., et al., 1994. Phase II studies of recombinant human interleukin-4 in advanced renal cancer and malignant melanoma. J. Immunother. Emphas. Immunol. 15, 147.
Micheau, O., Tschopp, J., 2003. Induction of TNF receptor I-mediated apoptosis via two sequential signaling complexes. Cell 114, 181.
Miyoshi, H., Smith, K.A., Mosier, D.E., Verma, I.M., Torbett, B.E., 1999. Transduction of human CD34+ cells that mediate long-term engraftment of NOD/SCID mice by HIV vectors. Science 283, 682.
Nathan, D.M., Angus, P.W., Gibson, P.R., 2006. Hepatitis B and C virus infections and anti-tumor necrosis factor-alpha therapy: guidelines for clinical approach. J. Gastroenterol. Hepatol. 21, 1366.
Oh, P., Li, Y., Yu, J., Durr, E., Krasinska, K.M., Carver, L.A., Testa, J.E., Schnitzer, J.E., 2004. Subtractive proteomic mapping of the endothelial surface in lung and solid tumours for tissue-specific therapy. Nature 429, 629.
Schneeweiss, S., Setoguchi, S., Weinblatt, M.E., Katz, J.N., Avorn, J., Sax, P.E., Levin, R., Solomon, D.H., 2007. Anti-tumor necrosis factor alpha therapy and the risk of serious bacterial infections in elderly patients with rheumatoid arthritis. Arthritis Rheum. 56, 1754.
Shibata, H., Yoshioka, Y., Ikemizu, S., Kobayashi, K., Yamamoto, Y., Mukai, Y., Okamoto, T., Taniai, M., Kawamura, M., Abe, Y., Nakagawa, S., Hayakawa, T., Nagata, S., Yamagata, Y., Mayumi, T., Kamada, H., Tsutsumi, Y., 2004. Functionalization of tumor necrosis factor-alpha using phage display technique and PEGylation improves its antitumor therapeutic window. Clin. Cancer Res. 10, 8293.
Shibata, H., Yoshioka, Y., Ohkawa, A., Minowa, K., Mukai, Y., Abe, Y., Taniai, M., Nomura, T., Kayamuro, H., Nabeshi, H., Sugita, T., Imai, S., Nagano, K., Yoshikawa, T., Fujita, T., Nakagawa, S., Yamamoto, A., Ohta, T., Hayakawa, T., Mayumi, T., Vandenabeele, P., Aggarwal, B.B., Nakamura, T., Yamagata, Y., Tsunoda, S., Kamada, H., Tsutsumi, Y., 2008. Creation and X-ray structure analysis of the tumor necrosis factor receptor-1-selective mutant of a tumor necrosis factor-alpha antagonist. J. Biol. Chem. 283, 998.
Stanger, B.Z., Leder, P., Lee, T.H., Kim, E., Seed, B., 1995. RIP: a novel protein containing a death domain that interacts with Fas/APO-1 (CD95) in yeast and causes cell death. Cell 81, 513.
Szlosarek, P.W., Balkwill, F.R., 2003. Tumour necrosis factor alpha: a potential target for the therapy of solid tumours. Lancet Oncol. 4, 565.
Vandenabeele, P., Declercq, W., Beyaert, R., Fiers, W., 1995. Two tumour necrosis factor receptors: structure and function. Trends Cell Biol. 5, 392.
Vandenabeele, P., Declercq, W., Vercammen, D., Van de Craen, M., Grooten, J., Loetscher, H., Brockhaus, M., Lesslauer, W., Fiers, W., 1992. Functional characterization of the human tumor necrosis factor receptor p75 in a transfected rat/mouse T cell hybridoma. J. Exp. Med. 176, 1015.
Wajant, H., Pfizenmaier, K., Scheurich, P., 2003. Tumor necrosis factor signaling. Cell Death Differ. 10, 45.
Weiss, T., Grell, M., Siemienski, K., Muhlenbeck, F., Durkop, H., Pfizenmaier, K., Scheurich, P., Wajant, H., 1998. TNFR80-dependent enhancement of TNFR60-induced cell death is mediated by TNFR-associated factor 2 and is specific for TNFR60. J. Immunol. 161, 3136.
Xu, H., Sethi, J.K., Hotamisligil, G.S., 1999. Transmembrane tumor necrosis factor (TNF)-alpha inhibits adipocyte differentiation by selectively activating TNF receptor 1. J. Biol. Chem. 274, 26287.
Yamamoto, Y., Tsutsumi, Y., Yoshioka, Y., Nishibata, T., Kobayashi, K., Okamoto, T., Mukai, Y., Shimizu, T., Nakagawa, S., Nagata, S., Mayumi, T., 2003. Site-specific PEGylation of a lysine-deficient TNF-alpha with full bioactivity. Nat. Biotechnol. 21, 546.

doi:10.1016/j.jmb.2008.05.047 J. Mol. Biol. (2008) 380, 777–782

JMB

Available online at www.sciencedirect.com

ScienceDirect

ELSEVIER

COMMUNICATION

Organelle-Targeted Delivery of Biological Macromolecules Using the Protein Transduction Domain: Potential Applications for Peptide Aptamer Delivery into the Nucleus

Tomoaki Yoshikawa[1,2]†, Toshiki Sugita[1,2]†, Yohei Mukai[1,2], Natsue Yamanada[1,2], Kazuya Nagano[1,2], Hiromi Nabeshi[1,2], Yasuo Yoshioka[1,3], Shinsaku Nakagawa[2], Yasuhiro Abe[1], Haruhiko Kamada[1,3], Shin-ichi Tsunoda[1,3]* and Yasuo Tsutsumi[1,2,3]

[1]*Laboratory of Pharmaceutical Proteomics, National Institute of Biomedical Innovation, 7-6-8 Saito-Asagi, Ibaraki, Osaka 567-0085, Japan*

[2]*Graduate School of Pharmaceutical Sciences, Osaka University, 1-6 Yamadaoka, Suita, Osaka 565-0871, Japan*

[3]*The Center for Advanced Medical Engineering and Informatics, Osaka University, 1-6 Yamadaoka, Suita, Osaka 565-0871, Japan*

Received 5 March 2008; received in revised form 16 May 2008; accepted 21 May 2008
Available online 29 May 2008

Edited by J. Karn

Extensive effort is currently being expended on the innovative design and engineering of new molecular carrier systems for the organelle-targeted delivery of biological cargoes (e.g., peptide aptamers or biological proteins) as tools in cell biology and for developing novel therapeutic approaches. Although cell-permeable Tat peptides are useful carriers for delivering biological molecules into the cell, much internalized Tat-fused cargo is trapped within macropinosomes and thus not delivered into organelles. Here, we devised a novel intracellular targeting technique to deliver Tat-fused cargo into the nucleus using an endosome-disruptive peptide (hemagglutinin-2 subunit) and a nuclear localization signal peptide. We show for the first time that Tat-conjugated peptide aptamers can be selectively delivered to the nucleus by using combined hemagglutinin-2 subunit and nuclear localization signal peptides. This nuclear targeting technique resulted in marked enhancement of the cytostatic activity of a Tat-fused p53-derived peptide aptamer against human MDM2 (mouse double minute 2) that inhibits p53–MDM2 binding. Thus, our technique provides a unique methodology for the development of novel therapeutic approaches based on intracellular targeting.

Keywords: Tat; HA2; nuclear localization signal; intracellular targeting; peptide aptamer

Progress in molecular biological research on intractable diseases such as cancer is steadily increasing our knowledge of the mechanisms of malignant transformation occurring in tumor cells. However, the complexity of biological interactions makes it increasingly difficult to predict gene and protein functions as we proceed from the immediate metabolic pathway to the levels of the cell and organism. Especially at the cellular level, a variety of tools are available to determine protein function and to develop novel therapeutic approaches, including antisense, peptide modulators, proteins and the overexpression of wild-type or dominant-negative proteins. Small peptides might be able to complement these agents because of

T.S. and T.Y. contributed equally to this work.

*Corresponding author. Laboratory of Pharmaceutical Proteomics, National Institute of Biomedical Innovation, 7-6-8 Saito-Asagi, Ibaraki, Osaka 567-0085, Japan.
E-mail address: tsunoda@nibio.go.jp.

† T.S. and T.Y. contributed equally to this work.

Abbreviations used: MDM2, mouse double minute 2; PTD, protein transduction domain; HA2, hemagglutinin-2 subunit; NLS, nuclear localization signal; NLS–VENUS–Tat, VENUS protein with Tat, NLS and His tag; Tat–cargo, Tat-fused cargo; HA2–Tat, Tat-fused endosome-disruptive HA2 peptide; PM10–Tat, Tat-fused PM10; NLS–PM10–

their ability to recognize specific protein domains and thus to interfere with enzymatic functions or protein–protein interactions.[1] Furthermore, these peptides, designated "peptide aptamers," seem to be non-genotoxic and useful for adjunct chemotherapy. However, these approaches are often limited by an inability to effectively deliver the agents to the appropriate cellular location.

Because a prerequisite for their intracellular action is their delivery into cells, various intracellular delivery approaches, such as protein transduction technology with protein transduction domains (PTDs; e.g., Tat, Antp, VP22, Rev and so on), are currently undergoing intensive scrutiny.[2,3] However, protein transduction technology using PTDs has some disadvantages, one of which is the accumulation of PTDs or PTD-fused peptides in the endocytic compartment. We and others have reported that the main mechanism of protein transduction is penetration into cells by macropinocytosis and that therefore much of the material taken up remains entrapped in the macropinosomes.[4–7] Another disadvantage is that there is no technique for controlling the intracellular distribution of peptide aptamers such that their effects are extremely limited. For these reasons, it is important that peptide aptamers be delivered directly into specific cellular compartments. Because optimal approaches for overcoming these disadvantages have not yet been developed, high concentrations of PTDs or PTD-fused peptides must still be employed in order for the technology to function effectively.

With this in mind, we focused on developing intracellular targeting technology for peptide aptamers fused with Tat protein basic domain residues 47–57 (YGRKKRRQRRR) from human immunodeficiency virus-1 in the context of cancer therapeutics. We recently reported that survivin-targeted peptide aptamers (shepherdin) linked to the NH_2-terminal domain of the influenza virus hemagglutinin-2 subunit (HA2), which is a pH-dependent fusogenic peptide inducing lysis of membranes at low pH levels,[8,9] are efficiently released from macropinosomes. This approach succeeded in inducing the death of survivin-expressing malignant tumor cells.[10] Based on this previous study, here we devised a novel intracellular targeting technology using HA2 and nuclear localization signal (NLS) peptides for converting peptide aptamers into efficient research tools for cell biology and cancer therapeutics. We established for the first time that Tat-conjugated peptide aptamers can be selectively delivered to the nucleus by combining HA2 and NLS peptides. Furthermore, we evaluated the utility of our nuclear targeting method using p53-derived peptide from the human MDM2 (mouse double minute 2, also termed HDM2 in humans)-binding domain (residues 17–26: designated PM10), which is a peptide inhibitor of p53–MDM2 binding.[11] Recent reports suggested that inhibiting p53–MDM2 binding could reactivate the p53 pathway and induce growth-suppressive effects and cell cycle arrest of tumor cells as well as normal cells possessing wild-type p53.[11–17] Because the interaction of p53 and MDM2 takes place inside the nucleus, nuclear delivery of PM10 may potentiate the cytostatic effect of this agent. Indeed, we found that our nuclear targeting technique employing PTD, HA2 and NLS peptides markedly enhanced PM10-mediated cytostatic effects against A549 (human lung adenocarcinoma) and WI-38 (human embryonic fibroblast, lung-derived cell line) cells. These results indicate that our intracellular targeting techniques can deliver the cargo into the appropriate organelle and provide a unique research tool for cellular biology and the development of novel therapeutic approaches.

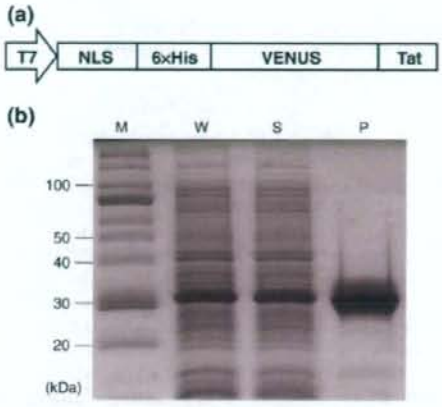

Fig. 1. Vector construction and SDS-PAGE analysis of NLS–VENUS–Tat. (a) Schematic of the NLS–VENUS–Tat region of T7 promoter-driven protein expression vector. The VENUS (variant of yellow fluorescent protein) DNA sequence was kindly provided by Dr. A. Miyawaki (RIKEN Brain Science Institute, Saitama, Japan). The NLS–VENUS–Tat DNA sequence was amplified by PCR. At the 5′ end, the primer sequence 5′-AA CTT TAA GAA GGA GAT ATA *CAT ATG* CCG AAA AAG AAA CGT AAA GTT ACC ATG GCT CAC CAC CAT CAC CAC CAT **GAC TAC AAA GAC GAT GAT GAC AAA** GAA GCT TAC GTG AGC AAG GGC GAG GAG CTG TT-3′ introduced an NdeI site (italics), an NLS (boldface) and a 6× His tag (underline); at the 3′ end, the primer sequence 5′-T TCC TTT CGG GCT TTG TTA GCA GCC *GAA TTC* TTA TTA **ACG GCG ACG CTG GCG ACG TTT TTT ACG ACC GTA** CTC GAG CTT GTA CAG CTC GTC CAT GCC GAG-3′ introduced an EcoRI site (italics) and a Tat sequence (boldface). The PCR product was digested with NdeI as well as EcoRI and inserted into pT7 vector, under the control of the T7 promoter. (b) The plasmid was transformed into *E. coli* BL21 Star (DE3) (Invitrogen, Carlsbad, CA), and cells expressing VENUS proteins were cultured at 25 °C, 250 rpm, for 6 h. The cell paste was then solubilized in a BugBuster Master Mix (Novagen, Darmstadt, Germany) and centrifuged. NLS–VENUS–Tat was recovered in the supernatant and purified by His-tag affinity purification and gel-filtration chromatography. SDS-PAGE analysis was performed under reducing conditions. Lane M, molecular weight standard; lane W, *E. coli* extracts prepared after induction of expression by IPTG; lane S, soluble fractions; lane P, purified proteins.

Tat-fused cargo can be selectively delivered to the nucleus by combining HA2 and NLS peptides

We constructed a VENUS protein (variant of yellow fluorescent protein) fused with Tat, NLS and His tag (NLS–VENUS–Tat) for use as an expression vector (Fig. 1a). NLS–VENUS–Tat was indeed expressed in *Escherichia coli* [BL21 Star (DE3)] after induction with IPTG. The level of expression of the NLS–VENUS–Tat protein was analyzed by SDS-PAGE in total cell lysates (Fig. 1b). Protein expression was specifically induced because we did not find substantially leaky expression of the recombinant protein (data not shown). Recombinant NLS–VENUS–Tat was produced almost entirely in the soluble fraction and had an apparent molecular mass of about 32 kDa under reducing conditions (Fig. 1b, lane S). Purification was carried out by lysis, and separation of the soluble fraction was carried out by centrifugation. This was then loaded onto a Ni^{2+} column for initial purification. The NLS–VENUS–Tat protein eluted from the Ni^{2+} column was more than 90% pure (Fig. 1b, lane P). The purity, apparent molecular mass and cellular internalization activity of the eluted NLS–VENUS–Tat proteins were established by SDS-PAGE and flow cytometry.

Numerous mechanistic studies have shown that Tat peptides rapidly permeate plasma membranes and translocate into the nucleus.[18–22] This mechanism is currently used to deliver proteins and nucleic acids to cell nuclei through covalent linkages of Tat and cargoes.[18] However, nuclear delivery has remained problematic and very limited, because endosome escape and nuclear transport of Tat-fused cargo (Tat–cargo) represent a passive rather than an active process. Indeed, in HeLa cells treated with NLS–VENUS–Tat alone, only punctate cytoplasmic fluorescence, and no fluorescence in the nucleus, was observed (Fig. 2). We had previously confirmed that Tat-fused VENUS co-localized in live cells to vesicles with FM4-64, which is a general endosome marker (data not shown). Furthermore, FAM (carboxyfluorescein) dye-fused Tat peptides also co-localized in FM4-64-positive endosomal vesicles (data not shown). Thus, these results indicated that much of the NLS–VENUS–Tat was entrapped within the endosomal vesicles, resulting in low levels of nuclear accumulation. It is therefore reasonable to propose that Tat–cargo alone cannot reach the targeted cellular compartment, especially the nucleus, and that the therapeutic effects of anticancer peptide aptamers are extremely limited for this reason. Therefore, we devised an active nuclear targeting technique using endosome-disruptive HA2 and SV40-derived NLS peptides.

Recently, we reported that co-treatment with Tat–cargo and the Tat-fused endosome-disruptive HA2 peptide (HA2–Tat) improved the endosome-escape ability and the tumor-killing activity of Tat-fused antisurvivin peptide aptamers.[10] Therefore, we hypothesized that NLS–VENUS–Tat can be delivered into the nucleus if NLS–VENUS–Tat can be engineered to escape from the endosomal vesicles into the cytosol by co-treatment with HA2–Tat. To investigate whether co-treatment with HA2–Tat does effectively improve the nuclear localization of NLS–Tat–cargo, we co-treated HeLa cells with NLS–VENUS–Tat and HA2–Tat and analyzed the intracellular localization of NLS–VENUS–Tat by confocal laser scanning

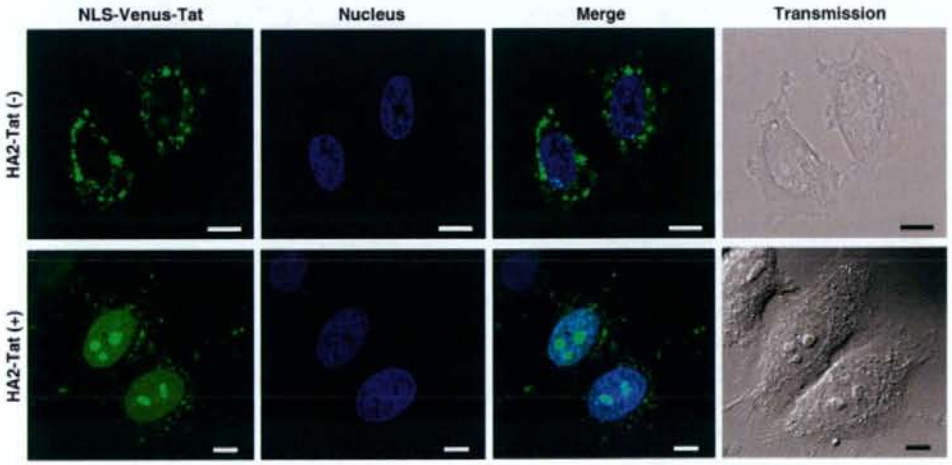

Fig. 2. Intracellular distribution of NLS–VENUS–Tat. HeLa cells were cultured on a Lab-Tek II Chambered Coverglass system (Nalge Nunc International) at 3.0×10^4 cells/well in MEM (minimum essential medium)-α supplemented with 10% fetal bovine serum and incubated for 24 h at 37 °C. Internalization of NLS–VENUS–Tat was performed as follows: HeLa cells were co-treated with NLS–VENUS–Tat (10 μM) with or without HA2–Tat (5 μM) in Opti-MEM I (Invitrogen) containing 100 ng/ml of Hoechst 33342 (Invitrogen). After incubation at 37 °C for 3 h, the medium was changed for a fresh medium and assessed by confocal laser scanning microscopy (Leica Microsystems GmbH, Wetzlar, Germany) without cell fixation. Scale bars in each photomicrograph represent 10 μm.

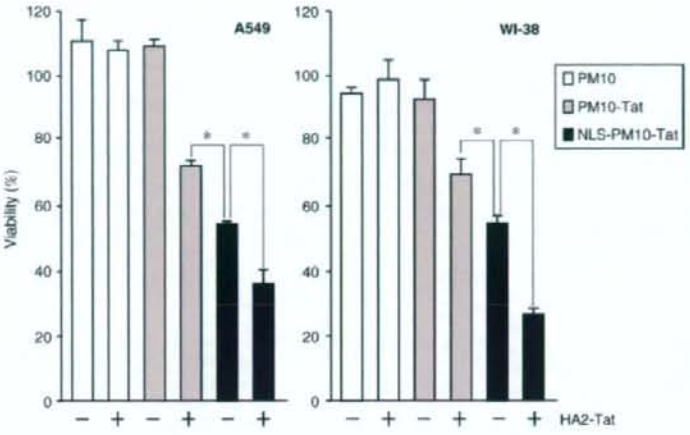

Fig. 3. Nuclear targeting potentiates the cytostatic effect of PM10. All peptides used in this study were purchased from GL Biochem Ltd. (Hiroshima, Japan) with confirmed purities >90% by HPLC and mass spectrography. The sequences of these peptides were GLFEAIEGFIENGWEGMIDGWYG**YGRKKRRQRRR** for HA2–Tat, ETFSDLWKLL for PM10, ETFSDLWKLL**YGRKKRRQRRR** for PM10–Tat and PKKKRKVETFSDLWKLL**YGRKKRRQRRR** for NLS–PM10–Tat. Tat and NLS are shown in boldface and underlined, respectively. A549 or WI-38 cells were seeded into 96-well tissue culture plates (Nalge Nunc International) at 1.0×10^4 cells/well. After incubation for 24 h at 37 °C, the cells were treated with PM10, PM10–Tat or NLS–PM10–Tat at 6 μM (for A549 cells) or 12 μM (for WI-38 cells) in the presence or absence of HA2–Tat (5 μM). After 6 h (for A549 cells) or 24 h (for WI-38 cells), cell viability was determined with the use of WST-8 assay (Nakalai Tesque Inc., Kyoto, Japan) according to the manufacturer's protocol. Data are presented as the mean±SD of triplicate assays. Statistical treatment of the data was performed according to Student's *t* test for two populations (*$p<0.01$).

microscopy (Fig. 2). Co-treatment of HeLa cells with NLS–VENUS–Tat and HA2–Tat resulted in nuclear localization of VENUS, co-localized with Hoechst 33342-stained nuclei. This finding documents that Tat-cargo can be selectively delivered to the nucleus by using HA2 and NLS peptides. Although several groups have attempted to deliver macromolecular drugs to specific organelles, they used PTDs conjugated only with an organelle-targeting signal, such as NLS or mitochondria-targeting signal.[23,24,25] Our data revealed that NLS–VENUS–Tat was entrapped within the endosomal vesicles, with no detectable fluorescence derived from VENUS found in the nucleus. This indicates that organelle targeting by signal-fused PTD–cargo alone does not allow efficient migration into the targeted organelle in the absence of an endosome-escape strategy. Although the influence of the use of different cell types, fluorescent dye, cargo, incubation time and so on could not be excluded as contributing to targeting inability, we found that nuclear transport efficiency could be augmented by combining PTD, HA2 and NLS peptides. Furthermore, our results imply that macromolecules could be delivered into other organelles, such as mitochondria, endoplasmic reticulum and peroxisomes, using different organelle-targeting signal sequences. To this end, we are currently developing novel intracellular drug delivery systems that can target macromolecules into different organelles in a manner analogous to our nuclear targeting techniques.

Nuclear targeting enhances the cytostatic activity of anti-MDM2 peptide aptamer

Next, we tested the utility of our nuclear targeting method using the MDM2-binding peptide aptamer, PM10, which is a p53-derived peptide corresponding to a sequence within the MDM2-binding domain. Kanovsky *et al.* reported that PTD-mediated intracellular delivery of PM10 could reactivate p53 and induce p53-mediated apoptosis of tumor cells with wild-type p53.[11] Under physiological conditions, growth-suppressive and proapoptotic activity of p53 is inhibited by MDM2, which binds p53 and negatively regulates its activity and stability.[16] Recent reports indicated that prevention of p53–MDM2 binding activates the p53 signaling pathway and induces p53-dependent apoptosis in cancer cells possessing wild-type p53.[12,14,15] In addition, the abrogation of p53–MDM2 binding mediates a cytostatic effect and cell cycle arrest in proliferating normal cells.[13,15,17] Because PM10 seems to bind nuclear-localized MDM2 and inhibits MDM2-inducible ubiquitination and degradation of p53, we hypothesized that the nuclear targeting method using HA2 and NLS peptides would enhance its cytotoxicity. To test this, we investigated the effects of treatment with PM10 on cell viability using A549 (human lung adenocarcinoma) and WI-38 (human lung-derived embryonic fibroblast) cells, which possess wild-type p53 (Fig. 3). In A549 and WI-38 cells treated with PM10, Tat-fused PM10 (PM10–Tat) grew vigorously. However, co-treatment with HA2–Tat and PM10–Tat together markedly inhibited A549 and WI-38 cell growth. Furthermore, A549 and WI-38 cells co-treated with HA2–Tat and NLS-fused PM10–Tat (NLS–PM10–Tat) showed greater growth inhibition compared with those treated with NLS–PM10–Tat alone. According to a report from the developers of PM10, although transduction of PTD-fused PM10 (PM10-PTD) into cancer cells could induce tumor cell death *in vitro* and *in vivo*, a high concentration of PM10-PTD was required to see an effect on cancer

cells.[11,26] In contrast, our nuclear targeting technique using PTD, HA2 and NLS peptides markedly enhanced the nuclear localization of the cargo and the PM10-mediated cytostatic effect at low concentrations of PM10. To the best of our knowledge, this is the first report that nuclear targeting of MDM2-binding peptide aptamers can lead to augmentation of cytostatic activity.

In the present study, we aimed to develop a novel cancer therapeutic approach by controlling apoptotic pathways using peptide-based drugs. Recently, the use of intracellular antibodies (intrabodies) directed to a specific target antigen present in the cell has also been suggested as a therapeutic lead to control the apoptotic pathway.[27,28] Our organelle-targeting strategy does seem able to deliver intrabodies directly to the specific organelle in which disease-related proteins reside. Furthermore, we have generated antibodies for various targeted antigens using a non-immune phage scFv library.[29] Thus, we are also currently developing a novel approach to intracellular therapy combining an organelle-targeting strategy and antibody engineering.

Acknowledgements

This study was supported in part by Grants-in-Aid for Scientific Research (20790156) from the Ministry of Education, Culture, Sports, Science and Technology of Japan; in part by a Health and Labor Sciences Research Grant from the Ministry of Health, Labor and Welfare of Japan; in part by a Grant for Industrial Technology Research Program (03A47016a) from the New Energy and Industrial Technology Development Organization of Japan; and in part by funding from the Takeda Science Foundation.

References

1. Mendoza, F. J., Espino, P. S., Cann, K. L., Bristow, N., McCrea, K. & Los, M. (2005). Anti-tumor chemotherapy utilizing peptide-based approaches—apoptotic pathways, kinases, and proteasome as targets. *Arch. Immunol. Ther. Exp.* **53**, 47–60.
2. Dietz, G. P. & Bahr, M. (2004). Delivery of bioactive molecules into the cell: the Trojan horse approach. *Mol. Cell. Neurosci.* **27**, 85–131.
3. Chauhan, A., Tikoo, A., Kapur, A. K. & Singh, M. (2007). The taming of the cell penetrating domain of the HIV Tat: myths and realities. *J. Controlled Release*, **117**, 148–162.
4. Fretz, M., Jin, J., Conibere, R., Penning, N. A., Al-Taei, S., Storm, G. *et al.* (2006). Effects of Na^+/H^+ exchanger inhibitors on subcellular localisation of endocytic organelles and intracellular dynamics of protein transduction domains HIV-TAT peptide and octaarginine. *J. Controlled Release*, **116**, 247–254.
5. Wadia, J. S., Stan, R. V. & Dowdy, S. F. (2004). Transducible TAT-HA fusogenic peptide enhances escape of TAT-fusion proteins after lipid raft macropinocytosis. *Nat. Med.* **10**, 310–315.
6. Sugita, T., Yoshikawa, T., Mukai, Y., Yamanada, N., Imai, S., Nagano, K. *et al.* (2008). Comparative study on transduction and toxicity of protein transduction domains. *Br. J. Pharmacol.* **153**, 1143–1152.
7. Kaplan, I. M., Wadia, J. S. & Dowdy, S. F. (2005). Cationic TAT peptide transduction domain enters cells by macropinocytosis. *J. Controlled Release*, **102**, 247–253.
8. Han, X., Bushweller, J. H., Cafiso, D. S. & Tamm, L. K. (2001). Membrane structure and fusion-triggering conformational change of the fusion domain from influenza hemagglutinin. *Nat. Struct. Biol.* **8**, 715–720.
9. Skehel, J. J., Cross, K., Steinhauer, D. & Wiley, D. C. (2001). Influenza fusion peptides. *Biochem. Soc. Trans.* **29**, 623–626.
10. Sugita, T., Yoshikawa, T., Mukai, Y., Yamanada, N., Imai, S., Nagano, K. *et al.* (2007). Improved cytosolic translocation and tumor-killing activity of Tat-shepherdin conjugates mediated by co-treatment with Tat-fused endosome-disruptive HA2 peptide. *Biochem. Biophys. Res. Commun.* **363**, 1027–1032.
11. Kanovsky, M., Raffo, A., Drew, L., Rosal, R., Do, T., Friedman, F. K. *et al.* (2001). Peptides from the amino terminal mdm-2-binding domain of p53, designed from conformational analysis, are selectively cytotoxic to transformed cells. *Proc. Natl. Acad. Sci. USA*, **98**, 12438–12443.
12. Vassilev, L. T., Vu, B. T., Graves, B., Carvajal, D., Podlaski, F., Filipovic, Z. *et al.* (2004). *In vivo* activation of the p53 pathway by small-molecule antagonists of MDM2. *Science*, **303**, 844–848.
13. Vassilev, L. T. (2004). Small-molecule antagonists of p53–MDM2 binding: research tools and potential therapeutics. *Cell Cycle*, **3**, 419–421.
14. Tovar, C., Rosinski, J., Filipovic, Z., Higgins, B., Kolinsky, K., Hilton, H. *et al.* (2006). Small-molecule MDM2 antagonists reveal aberrant p53 signaling in cancer: implications for therapy. *Proc. Natl. Acad. Sci. USA*, **103**, 1888–1893.
15. Shangary, S., Qin, D., McEachern, D., Liu, M., Miller, R. S., Qiu, S. *et al.* (2008). Temporal activation of p53 by a specific MDM2 inhibitor is selectively toxic to tumors and leads to complete tumor growth inhibition. *Proc. Natl. Acad. Sci. USA*, **105**, 3933–3938.
16. Kubbutat, M. H., Jones, S. N. & Vousden, K. H. (1997). Regulation of p53 stability by Mdm2. *Nature*, **387**, 299–303.
17. Efeyan, A., Ortega-Molina, A., Velasco-Miguel, S., Herranz, D., Vassilev, L. T. & Serrano, M. (2007). Induction of p53-dependent senescence by the MDM2 antagonist nutlin-3a in mouse cells of fibroblast origin. *Cancer Res.* **67**, 7350–7357.
18. Vives, E., Charneau, P., van Rietschoten, J., Rochat, H. & Bahraoui, E. (1994). Effects of the Tat basic domain on human immunodeficiency virus type 1 transactivation, using chemically synthesized Tat protein and Tat peptides. *J. Virol.* **68**, 3343–3353.
19. Vives, E., Brodin, P. & Lebleu, B. (1997). A truncated HIV-1 Tat protein basic domain rapidly translocates through the plasma membrane and accumulates in the cell nucleus. *J. Biol. Chem.* **272**, 16010–16017.
20. Potocky, T. B., Menon, A. K. & Gellman, S. H. (2003). Cytoplasmic and nuclear delivery of a TAT-derived peptide and a beta-peptide after endocytic uptake into HeLa cells. *J. Biol. Chem.* **278**, 50188–50194.
21. Caron, N. J., Quenneville, S. P. & Tremblay, J. P. (2004). Endosome disruption enhances the functional nuclear delivery of Tat-fusion proteins. *Biochem. Biophys. Res. Commun.* **319**, 12–20.

22. Lundberg, M., Wikstrom, S. & Johansson, M. (2003). Cell surface adherence and endocytosis of protein transduction domains. *Mol. Ther.* **8**, 143–150.
23. Shokolenko, I. N., Alexeyev, M. F., LeDoux, S. P. & Wilson, G. L. (2005). TAT-mediated protein transduction and targeted delivery of fusion proteins into mitochondria of breast cancer cells. *DNA Repair (Amst.)*, **4**, 511–518.
24. Del Gaizo, V. & Payne, R. M. (2003). A novel TAT-mitochondrial signal sequence fusion protein is processed, stays in mitochondria, and crosses the placenta. *Mol. Ther.* **7**, 720–730.
25. Matsushita, M., Tomizawa, K., Moriwaki, A., Li, S. T., Terada, H. & Matsui, H. (2001). A high-efficiency protein transduction system demonstrating the role of PKA in long-lasting long-term potentiation. *J. Neurosci.* **21**, 6000–6007.
26. Michl, J., Scharf, B., Schmidt, A., Huynh, C., Hannan, R., von Gizycki, H. *et al.* (2006). PNC-28, a p53-derived peptide that is cytotoxic to cancer cells, blocks pancreatic cancer cell growth *in vivo*. *Int. J. Cancer*, **119**, 1577–1585.
27. Wheeler, Y. Y., Kute, T. E., Willingham, M. C., Chen, S. Y. & Sane, D. C. (2003). Intrabody-based strategies for inhibition of vascular endothelial growth factor receptor-2: effects on apoptosis, cell growth, and angiogenesis. *FASEB J.* **17**, 1733–1735.
28. Williams, B. R. & Zhu, Z. (2006). Intrabody-based approaches to cancer therapy: status and prospects. *Curr. Med. Chem.* **13**, 1473–1480.
29. Imai, S., Mukai, Y., Nagano, K., Shibata, H., Sugita, T., Abe, Y. *et al.* (2006). Quality enhancement of the non-immune phage scFv library to isolate effective antibodies. *Biol. Pharm. Bull.* **29**, 1325–1330.

Laboratory of Pharmaceutical Proteomics[1], National Institute of Biomedical Innovation (NIBIO), Graduate School of Pharmaceutical Sciences[2], Center of Advanced Medical Engineering and Informatics[3], Osaka University, Osaka, Japan

Effect of protein properties on display efficiency using the M13 phage display system

S. Imai[1, 2], Y. Mukai[1, 2], T. Takeda[1], Y. Abe[1], K. Nagano[1, 2], H. Kamada[1, 3], S. Nakagawa[2], S. Tsunoda[1, 3], Y. Tsutsumi[1, 2, 3]

Received May 15, 2008, accepted May 21, 2008

Shin-ichi Tsunoda, Ph.D., Laboratory of Pharmaceutical Proteomics, National Institute of Biomedical Innovation (NIBIO), 7-6-8 Saito-Asagi, Ibaraki, Osaka 567-0085, Japan
tsunoda@nibio.go.jp

Pharmazie 63: 760–764 (2008) *doi: 10.1691/ph.2008.8132*

The M13 phage display system is a powerful technology for engineering proteins such as functional mutant proteins and peptides. In this system, it is necessary that the protein is displayed on the phage surface. Therefore, its application is often limited when a protein is poorly displayed. In this study, we attempted to understand the relationship between a protein's properties and its display efficiency using the well-known pIII and pVIII type phage display system. The display of positively charged SV40 NLS and HIV-1 Tat peptides on pIII was less efficient than that of the neutrally charged RGDS peptide. When different molecular weight proteins (1.5–58 kDa) were displayed on pIII and pVIII, their display efficiencies were directly influenced by their molecular weights. These results indicate the usefulness in predicting a desired protein's compatibility with protein and peptide engineering using the phage display system.

1. Introduction

Phage display systems have attracted much attention as the best technology to create functional mutant proteins and peptides ever since Smith et al. reported that random peptides could be displayed on the surface of filamentous M13 phage (Smith 1985). Many researchers have applied this system in attempts to create human antibodies and tissue-specific peptides (Schier et al. 1996; Maruta et al. 2003; Imai et al. 2006). Indeed, we have been successful in creating a useful mutant TNF to be used as a drug (Shibata et al. 2004; Yamamoto et al. 2003). Thus, the phage display system has a wide range of applications (Stich et al. 2003; Gourdine et al. 2005; Takashima et al. 2000).

Filamentous M13 phage has a circular single stranded DNA and takes the form of a long tube that consists of eleven kinds of proteins. This virus effectively proliferates upon infection of *E. coli* (Sidhu 2001; Bayer and Feigenson 1985; Kuhn 1987). In the phage display system, a fusion protein composed of target-molecule and coat protein is derived from a phagemid vector, and wild-type phage composition proteins (pI–pXI) are derived from a helper phage genome. These components can make phage libraries that display target-molecules by assembling within the periplasm of *E. coli*. The most useful characteristic of this system is that protein libraries can be displayed easily on the phage surface by inserting gene libraries within the phage genome. Target-molecules are obtained rapidly by the use of an *in vitro* affinity panning procedure that selects and amplifies specific phage clones (Smith 1985).

In the phage display system, target-molecules can be displayed on coat proteins (pIII, pVI, pVII, pVIII, pIX), though generally they are displayed on pIII or pVIII. Displaying 0–1 molecule per phage in the pIII type phage display system is suitable for isolating high-affinity molecules (Chasteen et al. 2006; Keresztessy et al. 2006). Alternatively, ten molecules can be displayed on a phage particle in the pVIII type phage display system to select low-affinity molecules (Verhaert et al. 1999; Kneissel et al. 1999; Lowman 1997).

As described, the phage display system is the most useful tool to create bioactive peptides and functional mutant proteins. However, because the efficiency of display is influenced by the properties of the target protein (molecular weight, electric charge, etc.), poor display often limits its application. Despite this problem, there is little research examining the relationship between display efficiency and a protein's properties. Thus, studies are warranted in order to apply the phage display system effectively. In this report, we prepared phages that displayed proteins of different molecular weights and electric charges to ascertain the relationship between display efficiency and protein properties.

2. Investigations, results and discussion

In this study we examined the relationship between protein properties (molecular weight, electric charge etc.) and the efficiency of display with pIII and pVIII coat proteins of the filamentous M13 phage display system (Fig. 1). To begin with, we prepared phages that displayed different electrically charged peptides on pIII (Fig. 2B) and evalu-

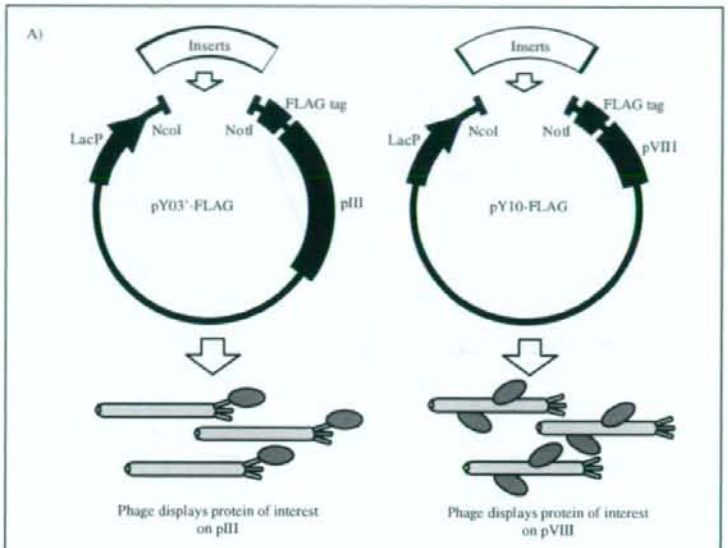

B)

Inserts	Molecular weight (Da)	pI
RGDS peptide (RGDS)	443	6.4
SV40 NLS peptide (PKKKRKV)	883	11.9
HIV-Tat peptide (YGRKKRRQRRR)	1,559	12.8
LacZ-α	11,000	5.2
anti-KDR scFv	25,000	5.0
Importin-α	58,000	5.1

Fig. 1:
Construction of phagemid vectors encoding different proteins or peptides.
A) Different inserts were cloned into pY03'-FLAG and pY10-FLAG phagemid vectors. Phage particles displaying proteins fused to pIII and pVIII were prepared from pY03'-FLAG and pY10-FLAG, respectively. B) Different inserts and their molecular weights

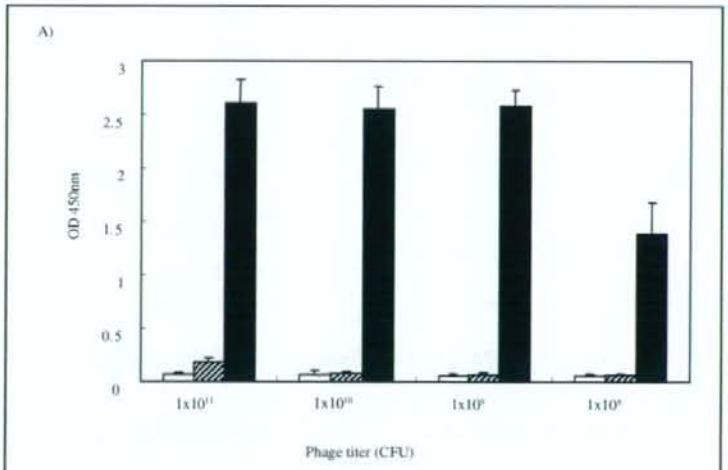

B)

	sequence	M.W. (Da)	pI
□ Tat peptide	YGRKKRRQRRR	1,559	12.8
■ SV40 NLS	PKKKRKV	883	11.9
■ RGDS peptide	RGDS	433	6.4

Fig. 2:
Influence of the efficiency of peptide-display by the ionic charge of peptides.
The efficiency of peptide-display on pIII was assessed by phage ELISA. Displayed peptides were fused to FLAG-tag – pIII on the phage particle and captured by immobilized anti-FLAG antibody. After washing, the number of captured phage was assessed by anti-M13 HRP conjugate. Two positively charged peptides (Tat peptide; □ and SV40 NLS; ■) and a neutral peptide (RGDS; ■) were used in this experiment (n = 3). Each data value represents the mean ± S.D. B) Sequences of displayed peptides and their pIs. Cationic amino acids are underlined. All pI values were calculated by Expasy Compute pI/Mw tool (http://au.expasy.org)

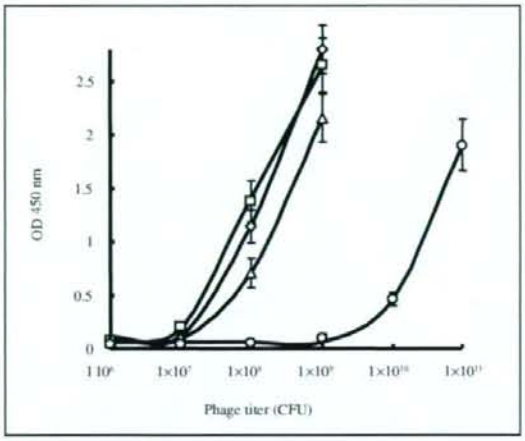

Fig. 3: Comparison of the efficiency of protein-display using pIII type phage display.
The efficiency of protein-display on pIII was assessed by phage ELISA. Proteins with different molecular weights (approximately 400–58,000 Da) were displayed on phage particle as pIII fusion proteins. This experiment was performed using the same method as Fig. 2 (n = 3). Each data value represents the mean ± S.D. □, RGDS-pIII phage; ◇, LacZ-pIII phage; △, scFv-pIII phage; ○, Importin-α-pIII phage

ated the relationship between electric charge and display efficiency using FLAG tagged ELISA (Fig. 2A). The display of positively charged SV40 NLS and HIV-1 Tat peptides were less efficient than that of the neutrally charged RGDS peptide. Generally, positively charged peptides are easy to adsorb onto various surfaces (Gaillard et al. 1999), and they repulse each other. Therefore, positively charged peptides may interfere with phage assembly in the periplasm.

Second, we examined the relationship between molecular weight and display efficiency again using FLAG tagged ELISA (Fig. 3). Because the display of positively charged sample was less efficient (Fig. 2), we used the neutrally charged proteins (pI 5.0–6.4) (MW 1.5–58 kDa) displayed on pIII to examine the influence of molecular weight on display. Phage displaying the low molecular weight RGDS peptide bound to anti-FLAG antibody at a concentration of 10^6–10^9 CFU. The higher molecular weight importin-α (58 kDa) displayed on the phage surface could not bind at the same concentration, needing 10^9–10^{11} CFU. In general, the amount of phage prepared by following the standard protocol was approximately 10^{12}–10^{13} CFU (Imai 2006). To create functional mutants using a phage library, it is desirable to use an amount of phage in excess (more than 100-fold) of the phage library (approximately 10^6–10^9 CFU). When proteins display on the phage surface efficiently, the experiment can proceed without bias. However, our result suggests that a phage library displaying high molecular weight proteins may be of low quality simply because the levels of the desired proteins are not sufficiently expressed for screening. This introduces a selection bias for those proteins that can be expressed at the proper level.

To examine the efficiency of pIII-display in greater detail, we quantified the number of molecules displayed on the phage surface by electrophoresis analysis using CsCl purified phage (Fig. 4). These results (Fig. 3, 4) demonstrate that the efficiency of RGDS peptide-display on pIII was the best (approximately 2 molecules/phage). The display efficiency decreased as the molecular weight of the target protein increased. Because the titer of all phages prepared in this experiment was determined, we suggested that the display of different molecular weight proteins did not affect the efficiency of phage-preparation (data not shown). Additionally, the proteins used in this experiment (RGDS, LacZ, scFv and importin-α) were expressed efficiently in *E. coli*. Therefore, we suggest that the efficiency with which a protein is displayed on pIII is directly related to its molecular weight.

Finally, we examined the efficiency of pVIII-display by Western blot and confirmed that it also decreased as the molecular weight increased (Fig. 5). Interestingly, this result shows that scFv (25 kDa) could be displayed on pVIII efficiently. Because the pVIII phage display system is generally believed to be limited in its application precisely by the molecular weight of displayed protein, many used it only for display of peptide libraries (Verhaert et al. 1999; Kneissel et al. 1999; Lowman 1997; Gaillard et al. 1999). However, our result suggests that the pVIII system could be applied to larger molecules. This could provide useful

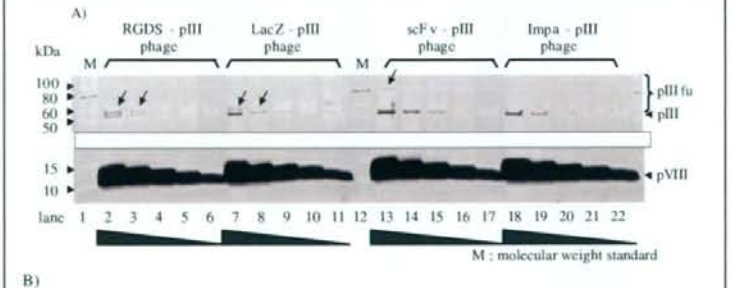

B)

	RGDS-pIII	LacZ-pIII	scFv-pIII	Impα-pIII
M.W. of displayed protein (kDa)	1.5	11	25	58
M.W. of pIII fusion protein (kDa)	52.5	62	76	109
Number of displayed proteins/phage	2.7	1.0	0.12	N.D.

N.D.; Not Detectable

Fig. 4:
Calculated quantity of pIII displayed proteins using Sypro® Ruby staining.
A) The efficiency of display on pIII was quantified using CsCl purifed phages. RGDS-pIII (lanes 2–6), LacZ-pIII (lanes 7–11), scFv-pIII (lanes 13–17) and Impα-pIII phage (lanes 18–22) were used in this experiment. Molecular weight standard was loaded in lanes 1 and 12. Starting from the left, 1×10^{13} vp, 3.3×10^{12} vp, 1.1×10^{12} vp, 3.7×10^{11} vp and 1.2×10^{11} vp were loaded. B) The number of displayed proteins per one phage particle was calculated by fluorescence image analysis. Fluorescence intensity was quantified by Typhoon image analyzer

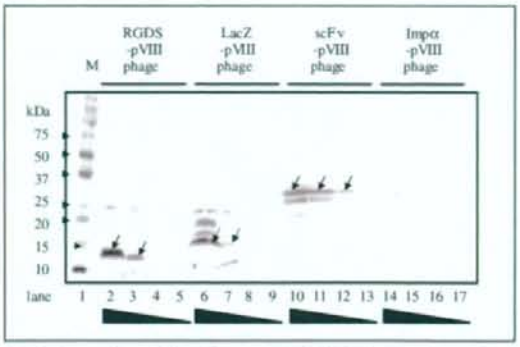

Fig. 5: Comparison of the efficiency of pVIII display protein on phage particles.
The efficiency of display on pVIII was assessed by anti-FLAG western blot. PEG-purified RGDS-pVIII (lanes 2–5), LacZ-pVIII (lanes 6–9), scFv-pVIII (lanes 10–13) and Impα-pVIII phage (lanes 14–17) were used in this experiment. Molecular weight standard was loaded in lane 1. Starting from the left, 1.5×10^{11} cfu, 5×10^{10} cfu, 1.7×10^{10} cfu and 5.5×10^{9} cfu were loaded

additional information by expanding the application of phage display systems to create various mutant proteins.

In this study, different kinds of sample peptides (SV40 NLS, HIV-1 Tat, RGDS) and proteins (RGDS, LacZ, scFv, importin-α) that could be readily expressed in *E. coli* were used as model molecules. The display of positively charged SV40 NLS and HIV-1 Tat peptides on pIII was less efficient than that of the neutrally charged RGDS peptide. When different molecular weight proteins (1.5–58 kDa) were displayed on pIII and pVIII, their display efficiencies were directly related to their molecular weights.

When comparing the efficiency of display between the four model proteins, additional factors (i.e. refolding efficiency, etc.) may account for the differences. These results show at least that the electric charge affected the efficiency of phage display and that high molecular weight proteins could not be displayed on the phage surface successfully. Recently, it was reported that improving the phagemid vector provided better efficiency of protein refolding in *E. coli* and enhanced protein display on the phage surface (Guo et al. 2003). Consequently many hope that the display efficiency of various molecules could be improved using this methodology. However, while this method improves the quality of fusion protein expression, it does not take into account the efficiency of protein assembly for the construction of phage particles. Therefore, it is still important to be able to predict the molecules that will be compatible for protein and peptide engineering using phage display by understanding the properties of this system as they were described in this report.

3. Experimental

3.1. Phagemid vectors and inserts

The pY03′-FLAG phagemid vector was modified from pCANTAB-5E (GE Healthcare Ltd.). To create this vector, the E-tag from the original vector was changed to a FLAG tag (DYKDDDDK). The pY10-FLAG phagemid vector was constructed by replacing the pIII gene in pY03′-FLAG with the pVIII gene. Genes encoding peptides (RGDS, HIV-Tat, SV40 NLS) were synthesized by Operon Biotechnologies Inc., USA. The lacZ-α gene had already been cloned into pY03′-FLAG and pY10-FLAG. The anti-KDR scFv gene was isolated from an optimized non-immune phage antibody library previously described (Imai et al. 2006). The human importin-α gene was amplified from a human bone marrow cDNA library (TAKARA Bio. Inc.). These inserts were digested and cloned into each phagemid vector.

3.2. Phage preparation

Phage was prepared by following a standard protocol. Briefly, phage particles were prepared from *Escherichia coli* (TG1 strain, Stratagene corporation) by co-infection with M13KO7 helper phage (Invitrogen Corporation). Amplified phage in culture media was roughly purified by PEG precipitation. Part of the purified phage was added to the TG1 bacteria, and the phage titer (cfu) was calculated by counting infected TG1 colonies. If necessary, additional purification using a CsCl gradient was performed as described below.

3.3. Phage ELISA

Immunoplates (Nalge Nunc International) were immobilized with anti-FLAG M2 antibody (Sigma-Aldrich Corporation) diluted to 5 μg/ml in bicarbonate buffer (Sigma-Aldrich Corporation). Plates were blocked with 2% block ace (Nakarai Tesque Inc.) for 2 h at 37 °C. Phage solution (PEG-purified) in 0.4% block ace was serially diluted and applied to the wells. After a 1 h incubation at room temperature, the binding phage was detected by anti-M13 HRP conjugate (GE Healthcare Ltd.).

3.4. Purification of phage particles under CsCl gradient

Amplified phage was purified by PEG precipitation. Phage pellets were resuspended in TBS buffer. CsCl powder (IWAI chemicals company) and additional TBS buffer were added to the phage solution up to 31%. After CsCl gradient ultracentrifugation at 400,000 × g at 5 °C for 20 h, the concentrated phage band was isolated. TBS (five volumes) was added to the purified phage and centrifuged again at 400,000 × g at 5 °C for 4 h to remove the CsCl. The obtained phage was resuspended in TBS and used for experiments.

3.5. Sypro Ruby staining

After purifying the phage under a CsCl gradient, the number of phage particles (vp/ml) was estimated from its absorbance according to the standard protocol. Serially diluted phage samples were resolved by SDS – poly acrylamide electrophoresis (SDS-PAGE). Gels were incubated in SYPRO® Ruby protein gel stain reagent (Pearce Biotechnology, Inc., USA) overnight at room temperature. After washing with wash buffer (10% methanol and 7% acetic acid) for 30 min, fluorescence was detected using the Typhoon Variable Image Analyzer (GE Healthcare Ltd.). The number of surface-displayed proteins was calculated from fluorescence intensity using ImageQuant TL software (GE Healthcare Ltd.) assuming that one phage particle contained five pIII coat proteins on its surface.

3.6. Anti-FLAG western blotting

SDS-PAGE was performed using serially diluted phage purified by PEG precipitation. Phage protein in the gel was transferred to PVDF membrane (GE Healthcare Ltd.) using the Hoefer TE 70 semi dry transfer unit (GE Healthcare Ltd.). Membranes were blocked in 4% block ace for 1 h. FLAG-tagged pVIII fusion protein was detected with anti-FLAG M2 antibody (Sigma-Aldrich Corporation) and anti-mouse IgG HRP conjugate (Sigma-Aldrich Corporation). After detection by ECL plus reagent (GE Healthcare Ltd.), its luminescence was quantitated using the LAS-3000 Lumi Imager (Fujifilm Corporation).

Acknowledgements: This study was supported in part by Grants-in-Aid for Scientific Research (No. 20015052) from the Ministry of Education, Culture, Sports, Science and Technology of Japan, by Health and Labor Sciences Research Grant from the Ministry of Health, Labor and Welfare of Japan, and in part by Research Fellowships for Young Scientists (No. 3608) from Japan Society for the Promotion of Science.

References

Bayer R, Feigenson GW (1985) Reconstitution of M13 bacteriophage coat protein. A new strategy to analyze configuration of the protein in the membrane. Biochim Biophys Acta 815: 369–379.

Chasteen L, Ayriss J, Pavlik P, Bradbury AR (2006) Eliminating helper phage from phage display. Nucleic Acids Res 34: e145.

Gaillard C, Flavin M, Woisard A, Strauss F (1999) Association of double-stranded DNA fragments into multistranded DNA structures. Biopolymers 50: 679–689.

Gourdine JP, Greenwell P, Smith-Ravin E (2005) Application of recombinant phage display antibody system in study of Codakia orbicularis gill proteins. Appl Biochem Biotechnol 125: 41–52.

Guo JQ, You SY, Li L, Zhang YZ, Huang JN, Zhang CY (2003) Construction and high-level expression of a single-chain Fv antibody fragment specific for acidic isoferritin in Escherichia coli. J Biotechnol 102: 177–189.

Imai S, Mukai Y, Nagano K, Shibata H, Sugita T, Abe Y, Nomura T, Tsutsumi Y, Kamada H, Nakagawa S, Tsunoda S (2006) Quality enhancement of the non-immune phage scFv library to isolate effective antibodies. Biol Pharm Bull 29: 1325–1330.

Keresztessy Z, Csosz E, Harsfalvi J, Csomos K, Gray J, Lightowlers RN, Lakey JH, Balajthy Z, Fesus L (2006) Phage display selection of efficient glutamine-donor substrate peptides for transglutaminase 2. Protein Sci 15: 2466–2480.

Kneissel S, Queitsch I, Petersen G, Behrsing O, Micheel B, Dubel S (1999) Epitope structures recognised by antibodies against the major coat protein (g8p) of filamentous bacteriophage fd (Inoviridae). J Mol Biol 288: 21–28.

Kuhn A (1987) Bacteriophage M13 procoat protein inserts into the plasma membrane as a loop structure. Science 238: 1413–1415.

Lowman HB (1997) Bacteriophage display and discovery of peptide leads for drug development. Annu Rev Biophys Biomol Struct 26: 401–424.

Maruta F, Parker AL, Fisher KD, Murray PG, Kerr DJ, Seymour LW (2003) Use of a phage display library to identify oligopeptides binding to the lumenal surface of polarized endothelium by ex vivo perfusion of human umbilical veins. J Drug Target 11: 53–59.

Schier R, Bye J, Apell G, McCall A, Adams GP, Malmqvist M, Weiner LM, Marks JD (1996) Isolation of high-affinity monomeric human anti-c-erbB-2 single chain Fv using affinity-driven selection. J Mol Biol 255: 28–43.

Shibata H, Yoshioka Y, Ikemizu S, Kobayashi K, Yamamoto Y, Mukai Y, Okamoto T, Taniai M, Kawamura M, Abe Y, Nakagawa S, Hayakawa T, Nagata S, Yamagata Y, Mayumi T, Kamada H, Tsutsumi Y (2004) Functionalization of tumor necrosis factor-alpha using phage display technique and PEGylation improves its antitumor therapeutic window. Clin Cancer Res 10: 8293–8300.

Sidhu SS (2001) Engineering M13 for phage display. Biomol Eng 18: 57–63.

Smith GP (1985) Filamentous fusion phage: novel expression vectors that display cloned antigens on the virion surface. Science 228: 1315–1317.

Stich N, Van Steen G, Schalkhammer T (2003) Design and peptide-based validation of phage display antibodies for proteomic biochips. Comb Chem High Throughput Screen 6: 67–78.

Takashima A, Mummert M, Kitajima T, Matsue H (2000) New technologies to prevent and treat contact hypersensitivity responses. Ann N Y Acad Sci 919: 205–213.

Verhaert RM, Van Duin J, Quax WJ (1999) Processing and functional display of the 86 kDa heterodimeric penicillin G acylase on the surface of phage fd. Biochem J 342: 415–422.

Yamamoto Y, Tsutsumi Y, Yoshioka Y, Nishibata T, Kobayashi K, Okamoto T, Mukai Y, Shimizu T, Nakagawa S, Nagata S, Mayumi T (2003) Site-specific PEGylation of a lysine-deficient TNF-alpha with full bioactivity. Nat Biotechnol 21: 546–552.